ISSN 1063-7745, Crystallography Reports, 2006, Vol. 51, Suppl. 1, pp. S4–S11.

DIFFRACTION AND SCATTERING OF IONIZING RADIATIONS

Numerical Modeling of Optical Properties of a System of Two Zone Plates for Focusing Hard Synchrotron Radiation

V. G. Kohn[a], I. I. Snigireva[b], and A. A. Snigirev[b]

[a] Russian Research Centre Kurchatov Institute, pl. Akademika Kurchatova 1, Moscow, 123182 Russia

[b] ESRF, BP 220, F-38043 Grenoble, France

e-mail: kohn@kurm.polyn.kiae.su

Received December 26, 2005

Abstract—Results of numerical experiments on focusing of a monochromatic spherical wave by a system of two linear zone plates are reported. Calculations were performed for a photon energy of 12.3985 keV and zone plates with a radius of the first zone of 5 μm, a number of zones of 628, and an aperture of 250 μm. To calculate the Kirchhoff integrals, the double Fourier transform method was used and the fast Fourier transform procedure on a grid with a number of points $65\,536 = 2^{16}$ was applied. On the basis of the calculation results, a conclusion was drawn that two zone plates operate as one with a doubled phase shift in zones with a material if the longitudinal distance between them is smaller than 1/3 of the focus depth and the transverse displacement is smaller than 1/3 of the outermost zone width (the focus size). If the distance (displacement) exceeds the focus depth (size), the two zone plates operate independently, similar to refracting lenses with a set of different focusing orders, including the zero order. The nature of the moiré pattern at a transverse displacement of the zone plates is discussed.

PACS numbers: 61.10.Dp

DOI: 10.1134/S1063774506070029

1. INTRODUCTION

In recent years, much attention has been paid to the problem of obtaining submicron (and even nanometer) beams of hard synchrotron radiation using different focusing systems. Among many such systems, the most widespread are curved reflecting systems: grazing incidence mirrors [1], multilayer coatings [2] and crystals [3, 4], Fresnel zone plates (FZPs) [5], and compound refracting lenses (CRLs) [6, 7]. FZPs and CRLs are relatively similar in their properties. They do not change the beam direction; i.e., they are in-line devices. This circumstance makes it possible to easily combine them with other elements of an optical scheme. They focus coherent quasi-monochromatic radiation and make it possible to obtain both an ordinary image of an object (including the source) and the Fourier image. Finally, they have a limited aperture.

However, the mechanism of aperture limitation of FZPs and CRLs is radically different. A CRL aperture is restricted by the absorption of radiation in the lens material. For this reason, CRL is preferential for hard radiation with photon energies E above 30 keV. For the FZPs, absorption is insignificant, and the aperture is restricted by the impossibility of formation of very small zones with a sufficient etch depth. This problem is serious exactly for hard radiation with high photon energy. As a result, the FZP efficiency decreases proportionally to φ^2 at $\varphi < 1/2$, where φ is the phase shift in radians for zones with a material. Note that φ decreases inversely proportionally to E.

A system of two zone plates can be used to overcome the noted difficulty. In this case, different methods are possible. One of them consists in such a distribution of zones between two plates at which each second zone has a material [8]. In this case, the width of etched zones in each FZP is about a factor of 3 larger than the effective width of the outermost zone (and, therefore, the focus size) in a system consisting of two FZPs. This technique has made it possible to decrease the size of the outermost zone to about 10 nm. Another way consists in the maximum close alignment of two identical FZPs [9]. In this case, it is obvious that two such FZPs should operate as one FZP with a doubled phase shift in the zones with a material, in contrast to CRLs. Thus, application of this technique may significantly (by a factor of 4) increase the efficiency of a two-FZP system based on zone plates with a low efficiency.

Since absolute alignment is almost impossible in practice, the problem about the allowable limits of transverse and longitudinal displacements of two FZPs with respect to each other arises. Although an analytic theory of intensity distribution in a focus has been developed for one FZP, it is very difficult to construct such a theory for two FZPs at an arbitrary (in particular, small) distance between them and the corresponding calculations have not been made.

In this study, an analysis of the optical properties of a system of two FZPs is performed by the method of numerical simulation in the ideal schematic of experiment with a point source of monochromatic radiation. The calculation was performed for two linear FZPs with a total number of zones of 624 and an outermost zone size of 0.1 μm. Currently, computational abilities do not make it possible to perform calculations for round FZPs with such a large number of zones. However, we believe the results obtained to be applicable for round FZPs. In Section 2, the calculation formulas are given and method of calculation is described. In Section 3, the values of the parameters are given and the analysis of the calculation accuracy by comparison with the analytic theory for one FZP is performed. The results of the calculations of the optical properties of a system of two FZPs are presented in Section 4.

2. THEORY AND METHOD OF NUMERICAL CALCULATION

Calculation of the wave field of radiation in the inline experimental scheme is formally simple. Since synchrotron radiation is strongly polarized and, in addition, polarization does not affect the result, it is sufficient to consider a scalar field with an amplitude $E(x, y, z)$. The z axis is directed along the optical axis and corresponds to large distances (from a millimeter to several meters). The x and y axes are directed perpendicularly, and the units of measurement in these directions are micrometers. Since the scattering angle for X rays is very small, the paraxial approximation is used, in which a spherical wave is replaced with a cylindrical one. If a field is known at some point of the optical axis with the coordinate z_1, the transport of this field through free space to a point with the coordinate z_2 is described by the Kirchhoff integral [10]

$$E(x_2, y_2, z_2) = \int_{-\infty}^{\infty} dx_1 \int_{-\infty}^{\infty} dy_1 P_2(x_2 - x_1, y_2 - y_1, z_2 - z_1) E(x_1, y_1, z_1), \tag{1}$$

in which the Kirchhoff propagator in the paraxial approximation has the form

$$P_2(x, y, z) = P(x, z)P(y, z),$$
$$P(x, z) = (i\lambda z)^{-1/2}\exp(i\pi x^2/\lambda z). \tag{2}$$

Here, λ is the wavelength of monochromatic radiation.

Since numerical calculation in infinite limits is impossible, it is necessary to restrict the model region. To this end, an arbitrary field at the point z_1 can be written as

$$E(x_1, y_1, z_1) = T(x_1, y_1, z_1)P_2(x_1, y_1, z_1). \tag{3}$$

If a relatively thin object which is illuminated by a point source located on the optical axis is placed at the point z_1, this field form describes a real situation in which the function $T(x, y)$ is the object transmission function. In the widely used geometric-optics approximation, this function has the form $\exp(i\Phi(x, y) - M(x, y))$. Here, $\Phi(x, y)$ describes the phase shift along the beam directed parallel to the optical axis and transmitted through the object at the point with the coordinates x and y and $\exp(-M(x, y))$ describes the radiation absorption in the object material along the beam path. We will consider only the cases where an object has inhomogeneous structure inside a finite rectangular region with sizes X and Y, while beyond this region, the object transmission function is equal to a constant C. Then, with the use of the property of the Kirchhoff propagator, formula (1) can be rewritten as

$$E(x_2, y_2, z_2) = CP_2(x_2, y_2, z_2)$$
$$+ \int_{-X/2}^{X/2} dx_1 \int_{-Y/2}^{Y/2} dy_1 P_2(x_2 - x_1, y_2 - y_1, z_2 - z_1) W(x_1, y_1), \tag{4}$$
$$W(x_1, y_1) = E(x_1, y_1, z_1) - CP_2(x_1, y_1, z_1).$$

The constant C, in particular, can be zero if the object is placed in an opaque gap of finite size. Note that, if the constant C is set improperly or is zero, artifacts appear at the edges of the model region. The effect of artifacts on the object image can be avoided through selection of a the model region that is larger than the object. However, a more exact result can be obtained by using a correct value of the constant C. Note also that the constant phase factor does not affect the intensity. Therefore, the object transmission function can always be chosen so that the constant is a real number. At the same time, uniform absorption in objects can be taken into account explicitly and only such object transmission functions for which $C = 1$ can be considered.

If all objects have a homogeneous uniform structure along the y axis, the calculation formula is simplified and takes the form $E(x, y, z) = P(y, z)E(x, z)$ and

$$E(x_2, y_2) = CP(x_2, z_2)$$
$$+ \int_{-X/2}^{X/2} dx_1 P(x_2 - x_1, z_2 - z_1) W(x_1), \tag{5}$$
$$W(x_1) = E(x_1, z_1) - CP(x_1, z_1).$$

During calculation of the system of two FZPs located successively along the optical axis, it is sufficient to apply formula (5) successively two times. In this case, the field directly behind the first FZP at the point z_1 is equal to $T_{zp}(x)P(x, z_1)$ and the field directly behind the second FZP at the point z_2 is equal to $T_{zp}(x)E(x, z_2)$, where the function $E(x, z_2)$ is obtained as the result of calculation by formula (5). Finally, the field $E(x, z_3)$ at the point of observation z_3 is obtained by repeated calculation by formula (5).

When calculating the zone plates, we disregarded the weak absorption in the zones and the presence of a homogeneous substrate. Therefore, the function $T_{zp}(x)$

was modeled as follows: $T_{zp}(x) = \exp(-i\varphi)$ in intervals $r_1(2k+1)^{1/2} < x < r_1(2k+2)^{1/2}$ and $T_{zp}(x) = 1$ in the intervals $r_1(2k)^{1/2} < x < r_1(2k+1)^{1/2}$ and $x > A/2$. Here k are integers in the interval from 0 to $K/2 - 1$, K is the total number of zones, r_1 is the radius of the first Fresnel zone, $A = 2r_1K^{1/2}$ is the FZP aperture, and φ is the actual phase shift in the zones with a material ($\varphi \le 0$). Note that the object transmission function defined above was modified to equate it to unity at the edges of the model region beyond the aperture.

The integral in formula (5) has the form of a convolution even for relatively small distances $z_2 - z_1$; until the image sizes exceed the sizes of the model region, it is convenient to calculate this integral by the double Fourier transform method. In the first stage, the Fourier transform $F_W(q)$ of the function $W(x)$ is calculated. Then, it is multiplied by the Fourier transform of the Kirchhoff propagator $F_P(q, z) = \exp(-i\lambda zq^2/4\pi)$ and the inverse Fourier transform of the product $F_W(q)F_P(q, z)$ of the two functions is found. The corresponding integrals were calculated by the fast Fourier transform method, which is described, for example, in [11]. To use this method, the integral over the region of size X is approximated by the sum of values of the integrand on the uniform grid of N points, multiplied by the grid step $\Delta_x = X/N$. The number of points N is chosen to be sufficiently large and equal to an integer power of 2; i.e., $N = 2^p$, where p is an integer. Accordingly, the coordinates of grid points in the x space are $x_n = \Delta_x(n + (1 - N)/2)$. The number of points in the q space coincides with the number of points in the x space, and the coordinates of these points are $q_m = \Delta_q(m + (1 - N)/2)$. The grid step in the q space is $\Delta_q = 2\pi/X$. It is easy to check that, in this case, the argument of the exponential of the Fourier transform is $q_mx_n \Rightarrow 2\pi mn/N$ and the necessary conditions are satisfied.

Numerical calculation of the diffraction of radiation from a zone plate with a large number of zones is a relatively difficult problem. The number of points in the x space should be sufficiently large to ensure exact description of the structure of the outermost zones and the focus. That is why the fast Fourier transform method is the best for this purpose. Calculation on the grid with N points includes $N\log_2N$ operations; hence, a very large number of points can be used. Calculation of the first Fourier transform generally causes no problems. For the overwhelming majority of actual objects, the function $F_W(q)$ decreases with increasing $|q|$ and is almost equal to zero at the edges of calculated grid. Therefore, calculation of the inverse Fourier transform likewise meets no problems. Unfortunately, for a zone plate, the behavior of the function $F_W(q)$ is different. At the same time, the function $F_P(q, z)$ does not decrease and, what is more, strongly oscillates at the edges of the calculation grid. The change in the phase of the function $F_P(q, z)$ at a step Δ_q at the edges of the calculation grid is $\Delta\phi = \pi\lambda zN/X^2$. At the focal length $z = F = r_1^2/\lambda$, the phase change can be expressed in terms of the aperture A and the number of zones K of the zone plate in the form $\Delta\phi = (\pi/4)(A/X)^2(N/K)$. The optimal values are $X \approx 3A$ and $N > 100$ K. It can be seen from this formula that the phase change is unacceptably high at these values of X and N. Accordingly, this circumstance results in the appearance of pronounced noise (random deviations from the average line) on the calculated curves at a small variation in the distance between the lenses or a transverse displacement.

The situation can be improved and the noise on the curves can be eliminated with the modified Fourier transform of the propagator that was previously integrated over the step of the calculation grid. Specifically, the computer program used the function with an additional factor in the form $F_P(q, z) = \exp(-i\lambda zq^2/4\pi)\sin(Bq)/Bq$, where $B = \lambda z\Delta_q/4\pi$. In the central region, i.e., at small values of $|q|$, this modification does not affect the form of the propagator. At the edges of the calculation grid, the function effectively decreases, thus leading to a decrease in the noise.

3. PARAMETERS OF THE NUMERICAL EXPERIMENT AND VERIFICATION OF ACCURACY

The calculation was performed for the photon energy $E = 12.3985$ keV ($\lambda = 1$ Å). The linear FZP had the radius of the first Fresnel zone $r_1 = 5$ μm and the total number of zones $K = 624$. Accordingly, the FZP aperture $A = 2r_1K^{1/2} = 250$ μm, the size of the outermost zone $\Delta r_K = 0.5r_1K^{-1/2} = 0.1$ μm, and the focal length $F = r_1^2/\lambda = 25$ cm. The distance from the point source to the FZP was $z_s = 50$ m; accordingly, the source image in the first-order focus was obtained at the distance $z_f = 25.1256$ cm behind the FZP. A grid consisting of 65536 = 2^{16} points with a step of 0.01 μm was used in calculations. In this case, the size of the model region was 655.36 μm, i.e., larger than the lens aperture by a factor of 2.6. Note that only 10 points fall in the focal region despite a very large number of points of the calculation grid.

If two identical FZPs having the phase shift $\varphi = \pi/2$ are ideally aligned to each other, we have one FZP with a phase shift of π. Exact calculation of the relative intensity distribution along the optical axis for one FZP can be performed by the formula

$$I(z) = \left|(1-i)(1-T)\sum_{k=1}^{K}(-1)^k G((2ck)^{1/2}) + T\right|^2,$$
$$c = F\frac{(z_s+z)}{z_s z}, \quad G(x) = \int_0^x dt \exp\left(i\frac{\pi}{2}t^2\right). \qquad (6)$$

Here, $T = \exp(i\varphi) = -1$ in the case under consideration. Intensity peaks (in focuses) arise at integer odd values of c. The first-order focus corresponds to $z = z_f$.

Two curves of relative intensity near the first-order focus in a 2-mm interval are shown for comparison in Fig. 1. The thin line shows the results of calculation by formula (6) for the parameters noted above. Squares show the calculation points taken from the general 2D (x, z) intensity distribution pattern by the fast Fourier transform method. It can be seen that the fast Fourier transform data are in good agreement with the results of exact calculation. However, the maximum value (in the focus) is slightly underestimated. This discrepancy is partially related to the limited range of integration in the q space. However, the main reason for this circumstance lies in the use of the modified propagator. Averaging of the propagator at the point of maximum (focus) independently of the function $F_W(q)$ is not quite justified, since both functions correlate well at the focus. Nevertheless, on the whole, this test shows that the use the fast Fourier transform method with the averaged propagator gives quite reasonable results.

In particular, the value of the focal depth sharpness (the width at half-maximum) is obtained with a very good accuracy. In this example, it is equal to $\Delta z_f = 0.71$ mm. An approximate analytic estimate for the focal depth sharpness can be obtained from (6) by replacing the Fresnel integrals with their asymptotic expansions and leaving of only the first two terms. This procedure leads to the formula

$$I(z) = \left|\frac{(T-1)}{\pi c^{1/2}}\sum_{k=1}^{K}\frac{\exp(i\pi k[c-1])}{k^{1/2}} + T\right|^2. \quad (7)$$

Considering the region near the nth-order focus, we will assume that $c = n + \varepsilon$, $\varepsilon \ll 1$. In this case, the argument in the exponent slowly varies with increasing k and the sum can be approximately replaced with an integral. As a result, leaving only the main contribution, we obtain

$$I_n(\Delta z) = \frac{4|T-1|^2 K}{\pi^2 n}\left|\frac{G((2K\varepsilon)^{1/2})}{(2K\varepsilon)^{1/2}}\right|^2. \quad (8)$$

This formula yields the estimate $I_{\max} = (16K/\pi^2 n)\sin^2(\varphi/2)$ for the maximum relative intensity at the nth order focus. The focal depth is obtained from the condition that the function $|G(x)|^2/x^2 = 0.5$ at $x = (2K\varepsilon)^{1/2} = 1.32$. For simplicity, we will consider the case of an infinitely distant source $z_s = \infty$. Then, $\Delta z_f = 1.7F/(Kn^2)$. In the first-order focus, we obtain the following estimates for the parameters noted above: $I_{\max} = 1018$ and $\Delta z_f = 0.68$ mm. These values are in good agreement with the results of the calculation.

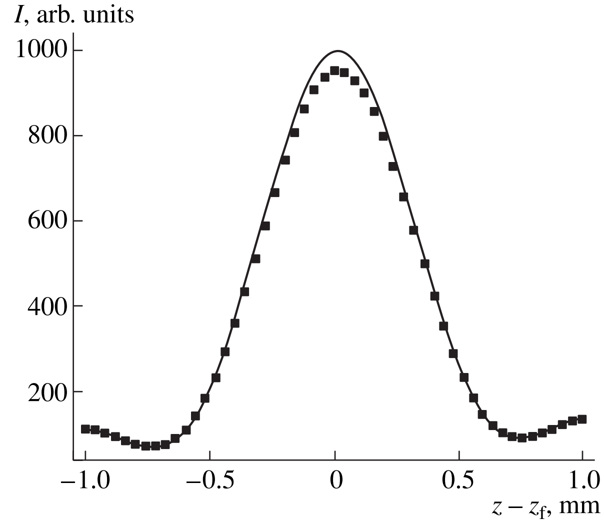

Fig. 1. Dependence of the relative intensity along the optical axis near the focus. Comparison of (squares) the fast Fourier transform data with (solid line) the results of the exact calculation.

4. RESULTS OF THE NUMERICAL EXPERIMENTS

It is well known that a zone plate focuses radiation in the first order similarly to a refracting lens with the same focal length. In particular, a zone plate satisfies the lens formula. A system of two zone plates located at some distance from each other also has focuses corresponding to the lens formula. However, in contrast to refracting lenses, two combined zone plates operate as one zone plate with a doubled phase shift. Moreover, with an increase in the distance between them, each of the two zone plates focuses some part of radiation independently of the other zone plate; i.e. two close focuses of lower intensity arise on the optical axis. Simultaneously, their common focus arises at a distance that is smaller by a factor of 2. This focus is an analogue of the common focus of two refracting lenses. In addition, other focuses arise.

The entire set of focal lengths satisfies the lens formula and can be obtained from consideration of the ray paths in two refracting lenses. The specificity of a zone plate consists in that it can be considered as a set of lenses with different focal lengths corresponding to different focus orders. The corresponding focal lengths can be denoted by two indices (n, m), which indicate the focus order in the first and second zone plates, respectively. For the distances to the source image counted from the first zone plate, we obtain the formula

$$z_f(n, m) = L + F_{2m}\frac{1 - LA_n}{1 + (F_{2m} - L)A_n}, \qquad A_n = \frac{1}{F_{1n}} - \frac{1}{z_s}. \quad (9)$$

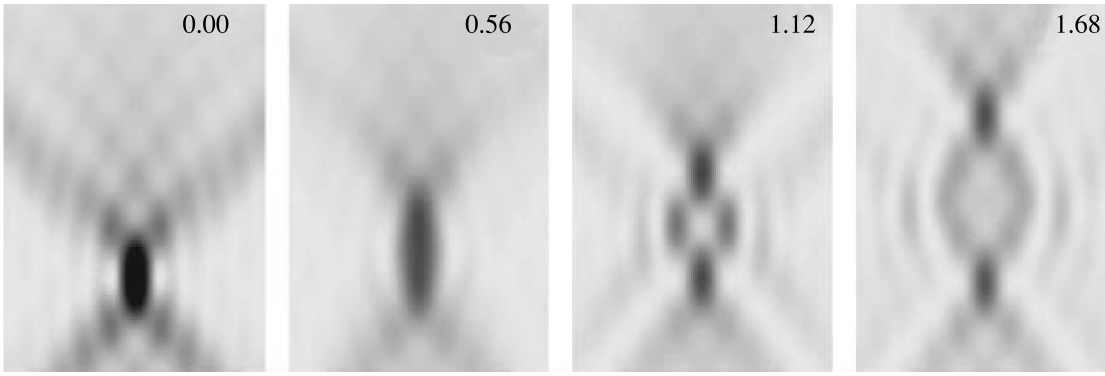

Fig. 2. 2D (x, z) distributions of the relative intensity near the focus at different longitudinal displacements of the second zone plate with respect to the first zone plate. The intensity is shown by linear scale of blackening from 0 (white) to 550 (black). The sizes of the model region in the horizontal and vertical directions are 1.08 μm and 4 mm, respectively. The longitudinal displacement L (in mm) is indicated in the images.

Here, L is the distance between two zone plates and $F_{1n} = F/n$ and $F_{2m} = F/m$ are the focal lengths of different orders in the first and second zone plates, respectively. In this case, along with the first, third, and higher orders, it is also necessary to take into account the zeroth order, for which the focal length is equal to infinity; i.e. $F_{10} = F_{20} = \infty$. From formula (9), in particular, we obtain $z_f(1, 0) = F/(1 - F/z_s)$ and $z_f(0, 1) = L + F/(1 - F/(z_s + L))$. At $L = 0$, these distances coincide and the common focus turns out to be more effective owing to the phase shift doubling. An increase in L should lead to the appearance of two focuses.

For more detailed analysis of the dynamics described above, calculation of a series of 2D (x, z) intensity distributions was performed at different L from 0 to 2 mm with a step of 0.08 mm. In these distributions, only 108 central points in an interval of 1.08 μm were chosen from the entire transverse calculation region. Since the distance $z_f(1, 0)$ is independent of L, it was used as a reference point for longitudinal distances. The interval over z from –1 to 3 mm was calculated. Figure 2 shows 4 of 26 images corresponding to the values L = 0, 0.56, 1.12, and 1.68 mm. The linear contrast from 0 (white) to 550 (black) used here is in best agreement with the results. It can be seen in Fig. 2 that, when the distance between the two zone plates with the phase $\varphi = \pi/2$ is equal to the focal depth, the maximum value sharply decreases from 950 to 350, whereas the focal depth sharpness increases. With a further increase in the distance between the two zone plates, two independent focuses arise. Between these focuses, a complex interference intensity distribution with a focus splitting perpendicularly to the optical axis is observed. The intensity distribution curves along the optical axis for all 26 values of L noted above are shown in Fig. 3. These data show that, within three steps (i.e., at L = 0.25 mm), the maximum value decreases by 15%. Thus, to obtain a higher efficiency in a system of two zone plates, the distance between them should not exceed 1/3 of the sharpness depth. The sharpness depth can be expressed in terms of the outermost zone width Δr_N of the zone plate. In this case, for the first-order focusing, the above-mentioned criterion can be written as

$$L < 2\frac{(\Delta r_N)^2}{\lambda}. \tag{10}$$

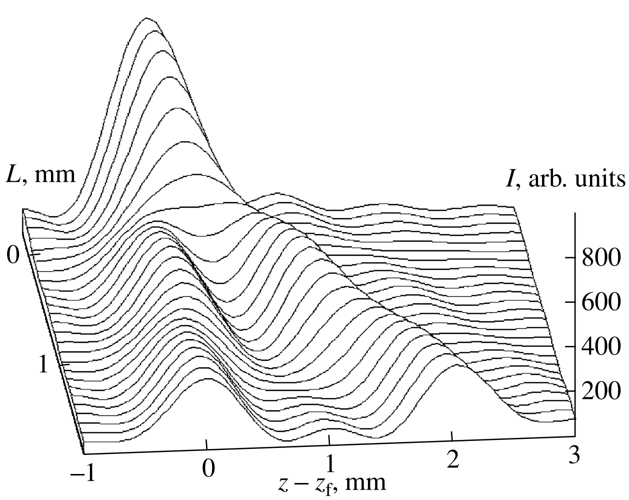

Fig. 3. Distribution of the relative intensity along the optical axis at different distances L between the two zone plates.

If each zone plate has a phase shift of π, the system of two zone plates has a phase shift 2π; therefore, it does not focus at all. It is of interest that, with an increase in the spacing between the zone plates, focuses at the distances $z_f(0, 1)$ and $z_f(1, 0)$ do not arise (this fact is confirmed by direct numerical calculation). The reason for this phenomenon is that the zone plates with a phase shift of π do not have a zero order. In this sense, they maximally correspond to refracting lenses. Nevertheless, such a system has a focus at the distance $z_f(1, 1) \sim$ 12.53 cm, which is about two times smaller than the initial focal length. In contrast to refracting lenses, this focus can exist only when there is some gap between the two zone plates, i.e., when they focus independently of each other. The results of the calculation of the transverse distribution of the relative intensity exactly at the focal length $z_f(1, 1)$ at different values of the distance L between the two zone plates are shown in Fig. 4. Note that the focal distance $z_f(1, 1)$ depends only slightly on L. As follows from the calculation, the double focus arises fairly rapidly with increasing L and has a significant magnitude even at $L = 0.1$ mm. However, at such a narrow gap between the plates, the secondary maxima are still not suppressed and there is interference. Therefore, the gap widths exceeding 0.25 mm are optimum. In other words, criterion (10) is valid again but with the opposite sign of inequality.

Note an important practical property of a system of two optimal zone plates with a relatively small distance between them. The distance at which their common focus is located is a factor of 2 smaller than the focal distance of a single zone plate. The size of the common focus is also smaller by a factor of 2, in complete agreement with the theory of a refracting lens, for which the focus size is $s = \lambda F/A$ (F is the focal length and A is the aperture). Thus, there is a fundamental possibility of obtaining a focus size smaller than the size of the outermost zone of a zone plate. However, the relative intensity in the focus (efficiency) in a system of two zone plates is smaller than that for a single zone plate. Although the zero order is absent, there are significant intensity losses in higher orders.

In addition, when two zone plates are aligned, it is important to know with what accuracy the transverse displacement S of the plates with respect to each other should be controlled. It is obvious, by analogy with the previous case of longitudinal displacement, that S should be smaller than the focus size by a factor of 3. To demonstrate this, let us consider again two zone plates with a phase shift of $\pi/2$, which have no gap between them ($L = 0$) but are displaced with respect to each other by S. The results of the calculation for this case at a distance of their common focus are shown in Fig. 5. It can be seen that at the displacement equal to 1/3 of the focus size, the intensity in the maximum decreases only by 10%. At displacements exceeding the focus size, the focus is split and each zone plate independently focuses the zero order of the other zone plate. This result is fairly unusual in the sense that the actual profile of the phase shift for a system of two zone plates has a very complex structure. Scattering occurs coherently, and we can only arbitrarily speak about the independence of two zone plates.

Note that when the transverse displacement S and the gap L are nonzero, the efficiency of the system of two zone plates decreases through both channels. Specifically, the focus expands both in the longitudinal and transverse directions at small values of S and L, whereas at large values each zone plate focuses according to its own geometric position. The calculations with nonzero S and L have been performed as well.

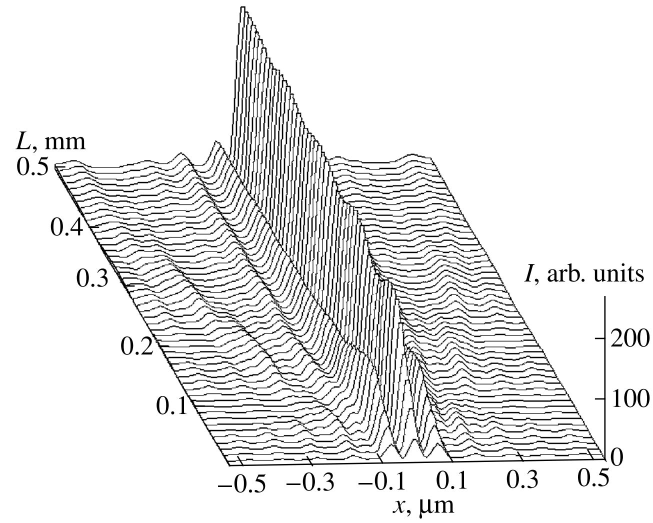

Fig. 4. Distribution of the relative intensity in the double focus (at the distance $z_f(1, 1)$) at different distances between the two identical zone plates with a phase shift of π in each plate.

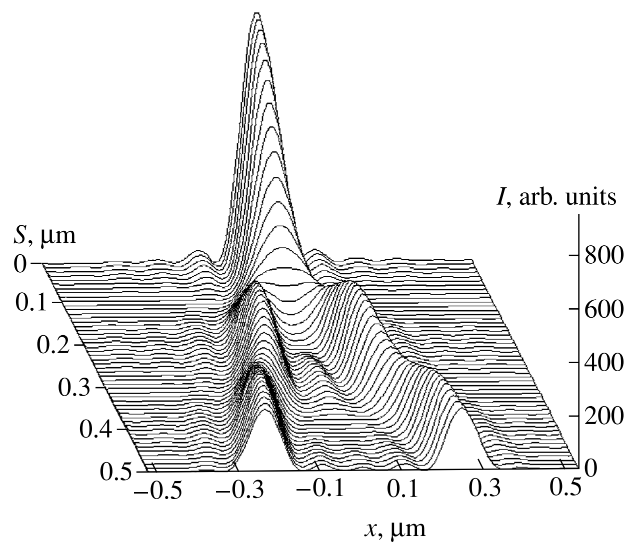

Fig. 5. Distribution of the relative intensity across the optical axis at different transverse displacements S between the two zone plates in the case of their close alignment ($L = 0$).

An interesting specific feature of the system of two zone plates is the presence of an interference (moiré) pattern in the aperture region of the zone plates at sufficiently large transverse displacements. At the focal length in the aperture region, the relative intensity is much lower than unity because a significant part of the intensity is collected at the focus. However, it is nonzero owing to the presence of higher- and zero-order focuses. For a system of two zone plates displaced in the transverse direction, the intensity distribution in the aperture region has a periodic structure of fringes with higher and lower intensities. The results of the calcula-

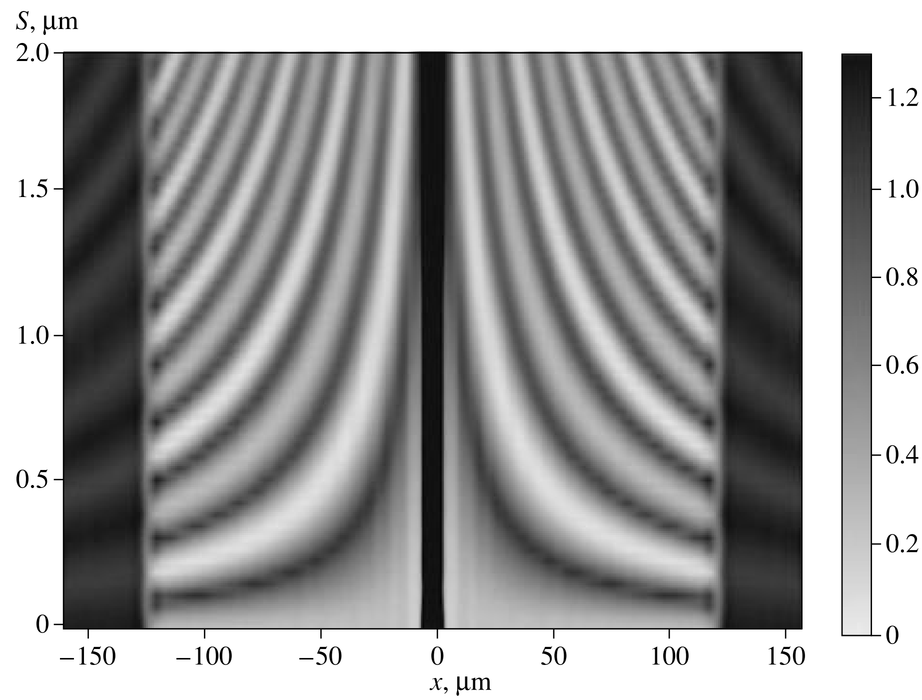

Fig. 6. Interference (moiré) pattern in the aperture region at a transverse displacement S between the two zone plates in the case of their close alignment ($L = 0$).

tion of the relative intensity in the aperture region for the system under consideration are shown in Fig. 6. To decrease the random noise in the table of points and the total number of points (i.e., 32 768 points), every 64 points were summed into one. The 512 points obtained were slightly smoothed by a convolution with the Gaussian function having a half-width equal to seven grid steps. It can be seen in Fig. 6 that the moiré pattern has a fairly sharp contrast. Note that the intensities in the minima are different. It is of interest that the deeper minima have tails outside the aperture in the form of a small decrease in the background intensity.

Apparently, the main source of the moiré pattern is the interference of the waves corresponding to the zero order of both zone plates. This suggestion is confirmed by the fact that period d of the moiré structure (the distance between neighboring maxima) obeys the law

$$d = \frac{r_1^2}{S}, \tag{11}$$

where S is the displacement of the zone plates and r_1 is the radius of the first zone. The moiré pattern directly behind the two zone plates in which phase-shifting zones are replaced with opaque zones obeys exactly the same law. The presence of a moiré pattern is very useful for the initial alignment of two zone plates during preparation of the experiment. However, this formula shows that, at a displacement equal to the outermost zone width, the distance between fringes is equal to the aperture. Therefore, the moiré pattern cannot be used to perform alignment with an error smaller than the outermost zone width.

5. CONCLUSIONS

It has been shown by numerical simulation that a system of two linear zone plates with the same structure can operate as a single zone plate with a higher efficiency if the longitudinal distance between the zone plates does not exceed 1/3 of the focal depth (equal to the focal length divided by the number of zones) and their transverse displacement does not exceed 1/3 of the outermost zone width (equal to the focus width). If the distance between the plates and their displacement exceed the focus sizes along and across the optical axis, each zone plate independently focuses the zero order of the aligned zone plate. It has been shown that the fast Fourier transform method is effective and sufficiently exact for numerical experiments with zone plates having a large number of zones.

ACKNOWLEDGMENTS

This study was supported by the Russian Foundation for Basic Research, project nos. 03-02-16971, 04-02-17363, and 05-02-16702.

REFERENCES

1. P. Kirkpatrick and A. V. Baez, J. Opt. Soc. Am. **38**, 766 (1948).

2. J. H. Underwood, T. W. Barbee, Jr., and C. Frieber, Appl. Opt. **25**, 1730 (1986).
3. T. Johansson, Z. Phys. **82**, 507 (1933).
4. F. Van Langeveide, D. K. Bowen, G. H. J. Tros, et al., Nucl. Instrum. Methods Phys. Res., Sect. A **292**, 719 (1990).
5. A. V. Baez, J. Opt. Soc. Am. **42**, 756 (1952).
6. A. Snigirev, V. Kohn, I. Snigireva, and B. Lengeler, Nature **384**, 49 (1996).
7. C. G. Schroer and B. Lengeler, Phys. Rev. Lett. **94**, 054 802 (2005).
8. W. Chao, B. D. Harteneck, J. A. Liddle, et al., Nature **435**, 1210 (2005).
9. J. Maser, B. Lai, W. Yun, et al., Proc. SPIE **4783**, 74 (2002).
10. V. G. Kohn, Phys. Scr. **56**, 14 (1997).
11. N. S. Bakhvalov, *Numerical Methods* (Nauka, Moscow, 1973; Mir, Moscow, 1977).

Translated by A. Madonov